New Proposal for the Bates P.A.C. Meeting, April 2-5, 1997

# Measurement of $A_x$ and $A_z$ Asymmetries in the Quasielastic $^3\vec{\mathrm{He}}(\vec{e}, e'd)p$ Reaction

H.-Y. Gao[1], J.-O. Hansen[1], R. Alarcon[2], J. Comfort[2], S.M. Dolfini[2], C. Mertz[2], A. Young[2], N. Kaloskamis[3], A. Karabarbounis[3], C. Papanicolas[3], C. Vellidis[3], M.B. Epstein[4], D.J. Margaziotis[4] A.J. Sarty[5], S. Williamson[6], R. Hicks[7], X.-D. Jiang[7], R. Miskimen [7], G. Peterson[7], J. Shaw[7], A.M. Bernstein[8], W. Bertozzi[8], J. Chen[8], D. Distler[8] G. Dodson[8], T.W. Donnelly[8], K. Dow[8], M. Farkhondeh[8], K. Fissum[8], S. Gilad[8], S. Kowalski[8], C. Kunz[8], M. Pavan[8], D. Rowntree[8], A. Skabelin[8], S.-B. Soong[8], J. Templon[8], D. Tieger[8], C. Tschalaer[8], W. Turchinetz[8], M. Wu [8], J.-G. Zhao[8], Z.-L. Zhou[8], T. Zwart[8], T.E. Chupp[9], K. Coulter[9], W. Lorenzon[9], T.B. Smith[9], R. Welsh[9], J. Zerger[9], J. Carlarco[10], F.W. Hersman[10], M.W. Holtrop [10], V. Pomeroy[10], T.P. Smith[10], S. Nagorny[11], L.B. Weinstein[12], A. Hotta[13], H. Miyase[13], T. Miura[13], T. Suda[13], and T. Tamae[13]

[1]*Argonne National Lab*, [2]*Arizona State University*, [3]*University of Athens-Greece*, [4]*California State University*, [5]*Florida State University*, [6]*University of Illinois-Urbana*, [7]*University of Massachusetts-Amherst*, [8]*LNS/Bates, Massachusetts Institute of Technology*, [9]*University of Michigan*, [10]*University of New Hampshire*, [11]*NIKHEF/KVI-The Netherlands*, [12]*Old Dominion University*, and [13]*Tohoku University-Japan*

| | | |
|---|---|---|
| Spokesperson(contact): | Z.-L. Zhou | (email: zzhou@mitlns.mit.edu) |
| Co-spokesperson: | R. Alarcon | (email: alarcon@bates.mit.edu) |
| Co-spokesperson: | W. Bertozzi | (email: bertozzi@mitlns.mit.edu) |
| Co-spokesperson: | T. Chupp | (email: chupp@mich.physics.lsa.umich.edu) |


**Abstract**

We propose to measure the quasielastic $A_x$ and $A_z$ asymmetries in the $^3\vec{\mathrm{He}}(\vec{e}, e'd)p$ reaction at $p_r$ = 20 and 110 MeV/c. The purpose of this measurement is to study the S′-wave contributions of the $^3$He ground-state wave function and the effects of isoscalar/isovector structure of the nuclear electromagnetic current. The experiment uses the high-pressure polarized $^3$He target from Experiment 88-25 and 750 MeV polarized electrons in the B-line in combination with the OOPS and OHIPS spectrometers.

| Description | Beam Hours | Energy($MeV$) | Current($\mu A$) | Duty Factor |
|---|---|---|---|---|
| $^3\vec{\mathrm{He}}(\vec{e}, e'd)p$ | 460 | 750-800 | 5-10 | 1 % |

# 1 Introduction

The $^3$He nucleus is the subject of considerable current interest. It is a calculable nuclear system where our understanding of nuclear structure can be precisely compared with data. In addition, it is generally thought that polarized $^3$He can serve as an effective polarized neutron target for experiments in nuclear [1] and particle [2] physics. Fundamental properties of the neutron such as its charge and spin distributions remain largely unconstrained experimentally. Thus, many experiments using polarized $^3$He targets are underway worldwide in large part motivated by measurement of neutron elastic form factors [3, 4, 5, 6, 7, 8, 9] and deep inelastic structure functions [10, 11, 12]. It is imperative to understand the ground state spin structure of the $^3$He nucleus to extract information on neutron structure from these measurements.

Non-relativistic Faddeev calculations [1, 13, 14] of the three body bound state predict that the following components dominate the $^3$He ground state wave function: a) a spatially symmetric $S$-state, accounting for $\sim$90% of the spin-averaged wave function and with the $^3$He spin entirely due to the neutron with the two protons in a spin singlet state; b) a $D$-state due to the tensor force accounting for $\sim$8% of the spin-averaged wave function and having the three nucleon spins dominantly oriented opposite to the $^3$He nuclear spin; c) a mixed-symmetry configuration of the nucleons, the S$'$-state, arising from spin-momentum correlations [15] and accounting for $\sim$2% of the spin-averaged wave function. All other components are predicted to be negligibly small.

The dominant component of the $^3$He wave function is the spatially symmetric S-wave. Here, the proton spins are in the singlet state and the $^3$He spin is solely carried by the neutron. This picture is supported by the near equality of the $^3$He and neutron magnetic moments ($\mu_{^3\mathrm{He}}$ = -2.12 nm and $\mu_\mathrm{n}$ = -1.91 nm). In this model polarized $^3$He would serve as an effective neutron target. Several experiments based on this concept have been proposed/approved with the goal to study the structure of the neutron (for example experiment E142 [10], E154 [11] at SLAC and HERMES [12] at DESY). Furthermore, experiments are in preparation at Bates [4, 8], Mainz [7], NIKHEF [6] and TJNAF [9] to measure the electromagnetic form factors of the neutron. However, it is clear that there are corrections to this naive picture. For example, it is expected that the protons in $^3$He are partly polarized due to the presence of the S$'$- and D-state components of the nuclear wave function. In addition, one has to understand the spin dependence of the reaction-mechanism effects such as final-state interactions (FSI) and meson-exchange currents (MEC).

The S$'$-state is a mixed symmetry S-wave configuration of the nucleons which indicates the deviation from symmetry due to the isospin-space correlations in the nuclear interaction. Results of a multitude of three-body calculations [16] show that its probability is strongly correlated with the binding energy as $\mathrm{P}_{\mathrm{S}'} \approx \mathrm{E_B}^{-2.1}$ ($\mathrm{E_B}$ in unit of MeV). The S$'$-state is an intriguing quantity: it obviously does not exist for $^2$H, for the three-body isospin doublet one has $\mathrm{P}_{\mathrm{S}'} \approx$ 1 - 1.5 %, whereas for $^4$He and heavier nuclei it is expected to be strongly suppressed ($\mathrm{P}_{\mathrm{S}'}$ < 0.1 %) due to the higher binding energies. The S$'$-state is an important quantity that deserves experimental investigation. For example, it is thought to be largely responsible for the difference in the charge radius between $^3$He and $^3$H. However, an important question is how one should go about in making precise measurements sensitive to such a small quantity.

This is best done by probing the electromagnetic structure of the $^3$He with medium- and/or high-energy electrons, since leptons can be treated as point-like particles and their electromagnetic interaction precisely computed in the framework of quantum electrodynamics. It has been shown [17, 18, 19] that the $^3\vec{\mathrm{He}}(\vec{e},e'p)pn$ and especially $^3\vec{\mathrm{He}}(\vec{e},e'd)p$ reactions will provide precise information on both the small S$'$- and D- components in the $^3$He wave function. The high level of current interest is shown by the fact that studies of the $^3\vec{\mathrm{He}}(\vec{e},e'p)pn$ and $^3\vec{\mathrm{He}}(\vec{e},e'p)d$ reactions have been proposed at NIKHEF [6], Mainz [20], TJNAF [21, 22] and Bates (BLAST) [8].

We propose a first study of the $^3\vec{\mathrm{He}}(\vec{e},e'd)p$ reaction at Bates with the high pressure $^3$He target of Exp 88-25 [4] and the OHIPS-OOPS spectrometer system. The measurements can be carried out in conjunction with Exp 88-25 inclusive scattering experiment. The polarized beam conditions at Bates are adequate to obtain precise data at low recoil momentum ($P_r \lesssim$ 150 MeV/c) for the $^3\vec{\mathrm{He}}(\vec{e},e'd)p$ reaction. In this kinematical region the D-state is highly suppressed and the beam-target asymmetries are sensitive to the interference of the S- and S$'$- states.

## 2 The $^3\vec{\mathrm{He}}(\vec{\mathrm{e}},\mathrm{e}'\mathrm{d})\mathrm{p}$ reaction

In the case of polarized beam and polarized target, the cross-section for the $^3\vec{\mathrm{He}}(\vec{e},e'd)p$ reaction has the general form (we follow here the notation of Laget [17]):

$$\frac{d\sigma(h,\vec{S})}{d\Omega_e dE_e d\Omega_d dp_d} = \frac{d\sigma_0}{d\Omega_e dE_e d\Omega_d dp_d} \cdot [1 + \vec{S}\cdot\vec{A}^0 + h(A_e + \vec{S}\cdot\vec{A})] \ , \tag{1}$$

where $\sigma_0$ is the unpolarized cross section, $\vec{S}$ is the spin of the target and h is the helicity of the electrons. $\vec{A}^0$, $A_e$ indicate the asymmetries produced by the polarization of only the target or only the beam, while $\vec{A}$ is the asymmetry when both the beam and the target are polarized. The target quantization axis is chosen to be along the direction of the momentum transfer. We will concentrate on $\vec{A}$ where only two asymmetries $A_{x,z}$ ($\vec{S}_x \perp \vec{q}$ and $\vec{S}_z \parallel \vec{q}$) are not equal to zero in coplanar geometry, *i.e.*, the spin is aligned in the scattering plane:

$$A_{x,z} = \frac{[d\sigma(+,+) + d\sigma(-,-)] - [d\sigma(+,-) + d\sigma(-,+)]}{[d\sigma(+,+) + d\sigma(-,-)] + [d\sigma(+,-) + d\sigma(-,+)]} \, . \tag{2}$$

Here, $(\pm,\pm)$ signs represent the beam helicities and the target spin projections along the quantization axis (x for A$_x$ and z for A$_z$). In this way with a 4 spin-flip sequence, possible systematic uncertainties and possible contributions from $\vec{A}^0$ and $A_e$ can be greatly suppressed.

It has been shown [18] that this single reaction provides information on both the small S$'$- and D- components in the $^3$He wave function. Also, the $^3\mathrm{He}(e,e'd)p$ channel is a source of information about isoscalar/isovector pieces of two-body electromagnetic currents at low recoil momentum, since one-body mechanisms are strongly suppressed near the deutron pole. In the $(e,e'p)$ channel the two-body currents become manifest only at high recoil momentum which makes it difficult to investigate them.

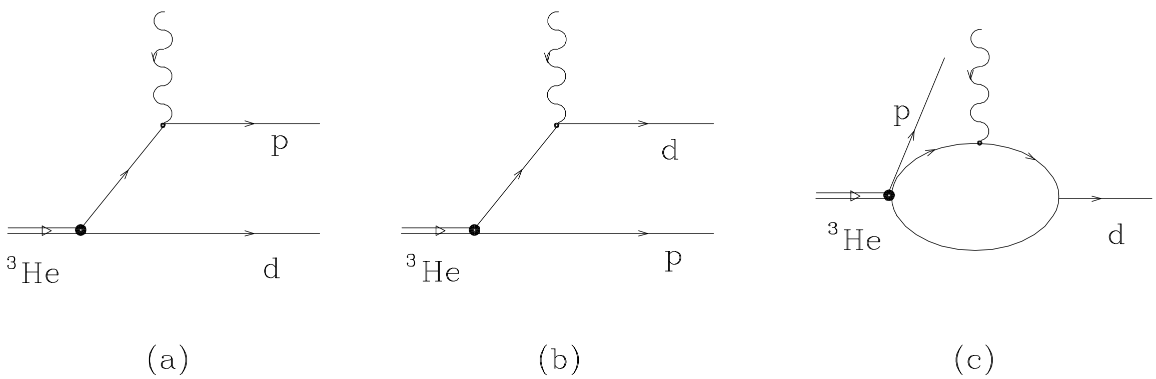


Figure 1: A few diagrams for illustration purpose. a) proton pole, b) deuteron pole corresponding to the quasi-deuteron model, (a) and b) together with $^3$He-pole and contact diagrams form the isoscalar current contributions), c) isovector current.

Fig. 1 shows a few diagrams for the $^3\mathrm{He}(e,e'd)p$ reaction. The first diagram with the proton pole corresponds to the plane-wave impulse approximation. The diagram with the deuteron pole corresponds to the quasi-deuteron model. The calculation includes the contact and $^3$He pole diagrams. For these diagrams the internal state of the pn-pair before and after the photoabsorption is the same. Thus, the isospin of the pn-pair does not change during photoabsorption and in this sense this current may be called an isoscalar current.

The isovector current is given by the totality of diagrams. In this case the internal state of the pn-pair before and after photoabsorption is different; hence in this case the isospin of the pn-pair changes during the photabsorption and this piece of the full current may be called an isovector current. For numerical calculations the $^3$He Faddeev wave functions for the Reid potential have been used [18].

For the $(e,e'p)$ reaction in quasi-elastic kinematics on the proton, the first diagram will dominate at low recoil momentum. Its amplitude may be factorized, and at low recoil momentum, where only the S-wave part of the vertex is retained, all information about nuclear dynamics will be cancelled in the ratio. Then the asymmetries will be given by only the proton form factors and the reaction $^3\vec{\mathrm{He}}(\vec{e},e'p)d$ provides no sensitivity on the S$'$- components, which manifest themselves only at small recoil momentum. Clearly, in the main S-wave configuration, one proton spin direction coincides with the neutron spin orientation and, as a result, coincides with the nuclear spin. Then the proton which absorbs the virtual photon in the $^3\mathrm{He}(e,e'p)d$ channel at low recoil momentum has a selected spin orientation opposite to the nuclear spin. In this case the polarized $^3$He is a simple polarized proton target.

For the $(e, e'd)$ reaction in quasi-elastic kinematics, it is the deuteron pole which is near the "physical" region and at low recoil momentum the contributions of one-body mechanisms will be strongly suppressed. Now the full amplitude will define both the isoscalar and isovector transitions. Due to the interference of the isoscalar and isovector transitions, the cancellation of the nuclear dynamics is impossible, and the asymmetries in the $^3\vec{\mathrm{He}}(\vec{e}, e'd)p$ channel will be sensitive to the S′- component.

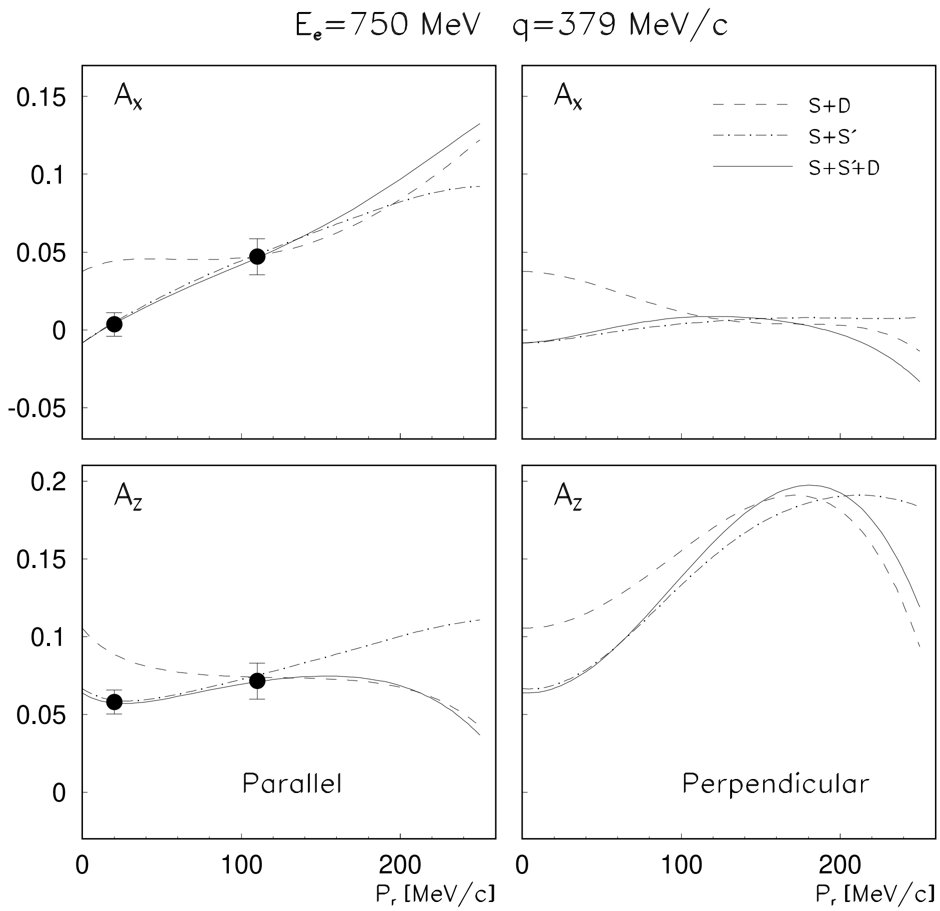


Figure 2: $A_x$ and $A_z$ Asymmetries for parallel $\vec{P}_r \| \vec{q}$ (left panel) and perpendicular $\vec{P}_r \perp \vec{q}$ (right panel) kinematics with a 750 MeV electron beam and a 30° scattering angle. The dashed, dash-dotted and solid curves represent the calculations with inclusions of S+D, S+S′ and S+S′+D waves in the $^3$He ground-state [23]. The circles represent our projected measurements.

In Fig. 2 the asymmetries $A_{x,z}$ for the $^3\vec{\mathrm{He}}(\vec{e}, e'd)p$ channel are plotted as functions of the recoil momentum for the parallel $\vec{P}_r \| \vec{q}$ (left panel) and perpendicular $\vec{P}_r \perp \vec{q}$ (right panel) kinematics at $E_e$ = 750 MeV and q=379 MeV/c. The large effects from S′- and D- components arise in the different regions of the recoil momentum. Note that, the calculations are from Dr. S. Nagorny [23] and the solid circle represent our proposed measurements.

We see also that at $100 < P_r < 120$ MeV/c there is practically no sensitivity of neither asymmetry to the S′- and D- components. Thus, this interval of recoil momenta may be used for examining the effects of FSI and the isoscalar/isovector current structure. In these calculations, it is evident that this interval is practically model independent, as it is determined only by the composition of the partial waves in the momentum distribution functions which are very similar for different realistic potentials up to 0.3 GeV/c.

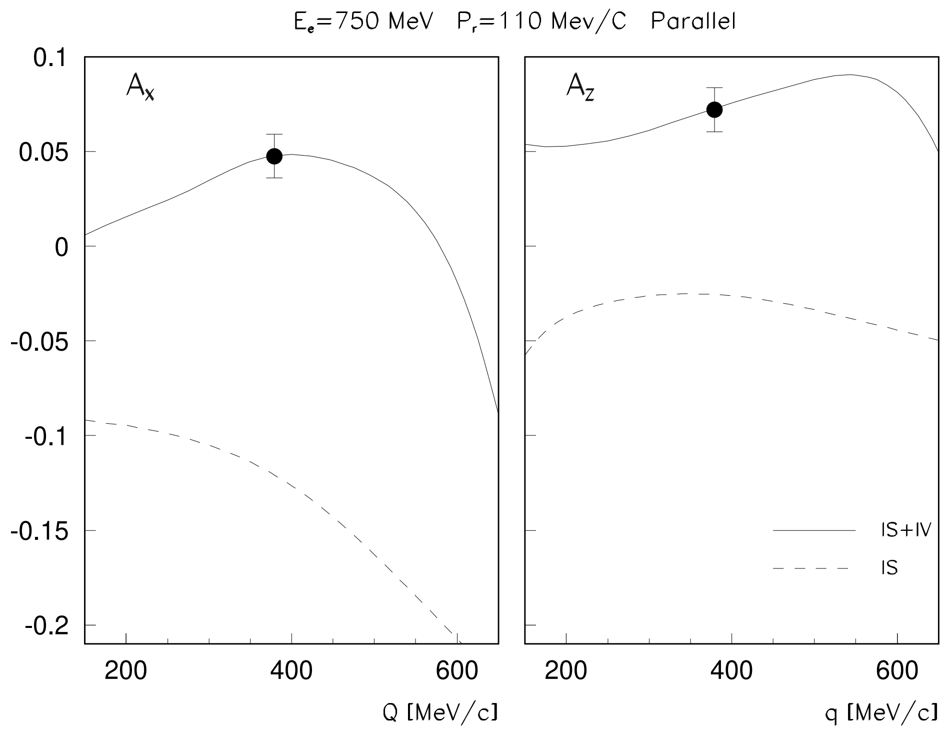


Figure 3: $A_x$ and $A_z$ Asymmetries as a function of the momentum transfer at a fixed recoil momentum ($P_r$ = 110 MeV/c) for parallel $\vec{P}_r \| \vec{q}$ kinematics with a 750 MeV electron beam. The solid (dashed) curve represents the calculations with the isoscalar and isovector current (only the isoscalar current) contributions [23]. The circles represent our projected measurements at $P_r = 110$ MeV/c, which are the same points as in Fig. 2 at $P_r = 110$ MeV/c for parallel kinematics.

In Fig. 3 the asymmetries $A_{x,z}$ for the ${}^3\vec{\mathrm{He}}(\vec{e}, e'd)p$ channel are plotted as functions of 3-momentum transfer at $P_r = 110$ MeV/c for the parallel $\vec{P}_r \| \vec{q}$ kinematics. Clearly, in this special kinematics the effects from nuclear dynamics and current structure are separated, since: 1) there is no sensitivity of $A_{x,z}$ to the small nuclear components and 2) there is strong sensitivity of both asymmetries to the structure of the nuclear current. Again, the calculations are from Dr. S. Nagorny [23] and the solid circles represent our proposed measurements, which are the same measurements as in Fig. 2 at $P_r = 110$ MeV/c for parallel kinematics.

Recent Bates measurements [24] show compelling evidence for the important role of the isovector current. Therefore, simultaneous measurements of $A_{x,z}$ at $P_r \simeq 110$ MeV/c region and $P_r \lesssim 50$ MeV/c will provide not only information on the important role of isovector current in the spin observables, but also a way to disentangle the contributions of the S$'$-component and the structure of nuclear electromagnetic currents.

Early studies of the unpolarized $^3$He$(e, e'd)p$ reaction at NIKHEF [25] indicate that the FSI effects in the cross-section can be as large as 20% for a momentum transfer of 380 MeV/c. Therefore, a spin-dependent measurement will also provide information for more rigorous calculations.

As shown in Fig. 2 and 3, we intend to concentrate only on the parallel $\vec{P}_r \| \vec{q}$ kinematics in this proposal. In general, more measurements can be done, for example, with the perpendicular kinematics where $\vec{P}_r \perp \vec{q}$ or even with the out-of-plane capability to measure A$_y$. Furthermore, simultaneous measurments can be done with the $^3\vec{\mathrm{He}}(\vec{e}, e'p)d$ , $^3\vec{\mathrm{He}}(\vec{e}, e'p)pn$ and/or $^3\vec{\mathrm{He}}(\vec{e}, e'p)X$ $(X = d, pn)$ reactions. However, we intend to limit the scope of discussion here.

# 3 Experiment

In this proposal, we propose measurements of A$_x$ and A$_z$ asymmetries in the $^3\vec{\mathrm{He}}(\vec{e}, e'd)p$ reaction. The measurements will be emphasized in two regions of the recoil momenta: P$_r$ $\lesssim$ 50 MeV/c where the effects of the S$'$- component are large and P$_r$ $\sim$ 110 MeV/c where the effects of the wave functions and the isoscalar/isovector structure of the nuclear electromagnetic currents can be disentangled. We plan to use the high pressure polarized $^3$He target from Exp 88-25 and the polarized electron beam in the B-line. The scattering electrons will be detected in OHIPS spectrometer in coincidance with the knock-out deuterons detected in OOPS sepectrometer(s). In order to continuously monitor the polarization of the beam and target, one OOPS will be used to detect elastically scattered electrons at a forward angle.

## 3.1 Detectors

Fig. 4 a) and b) show the layout of the detector configuration and the target spin orentations for the measurements of A$_x$ and A$_z$ asymmetries in the $^3\vec{\mathrm{He}}(\vec{e}, e'd)p$ reaction. All the directions are in the scattering (horizontal) plane.

In the detector configuration as shown in Fig. 4a), OHIPS is set at 30° scattering angle to detect the scattered electrons in coincidence with the knock-out deuterons in OOPS$^2$. With a beam energy of 750 MeV, this will give a momentum transfer of about 379 MeV/c. We intend to use only one OOPS to detect the deuterons along the momentum transfer direction to perform measurements for the parallel kinematics. We propose two measurements with one close to zero recoil momentum and the other at $P_r \sim 110$ MeV/c region. With only one OOPS, one can easily set it up at a short drift distance to significantly increase the angular acceptance. Also, as shown in Fig. 4a), OOPS$^1$ will be used to detect elastically scattered electrons at 20° angle to continueously monitoring the polarization of the beam and target.

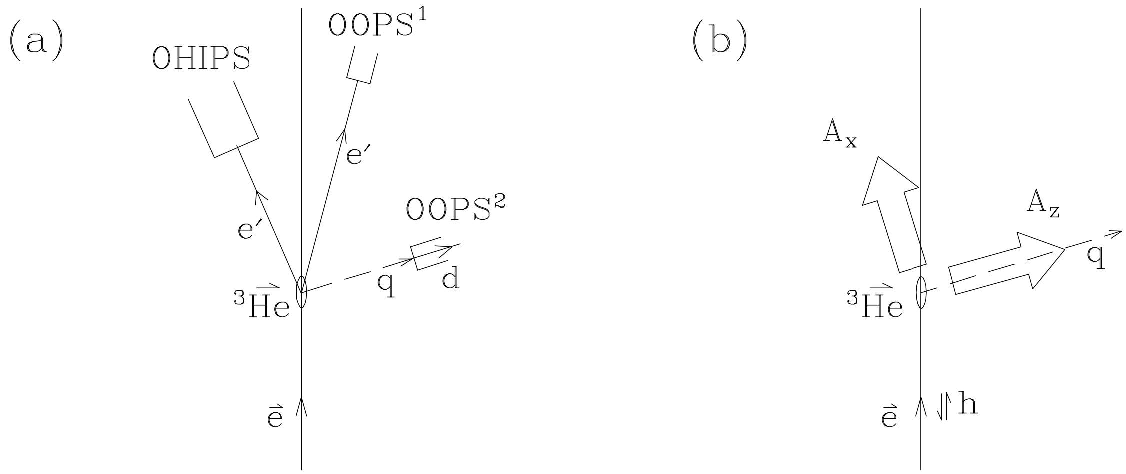


Figure 4: Schematic outline of the experimental configuration. a) OOPS[1] for detecting elastically scattering electrons and OHIPS-OOPS[2] configuration for the $^3\vec{\mathrm{He}}(\vec{e},e'd)$ in parallel kinematics. b) beam helicity and target polarization alignment for $A_x$ and $A_z$ asymmetries.

The short drift distance for OOPS is available without any technical difficulties, as same as for OHIPS. Preliminary calculations from the TURTLE simulation [26] of OOPS indicate that the momentum resolution at a 0.7 m drift distance is similar to the results obtained at 1.4 m drift distance. However, the performance with a short drift distance has to be determined through optics studies. Since OHIPS and OOPS have become the standard intrumentation in the B-line, such optics studies are anticipated in the near future.

In the proposed configuration, we can perform the measurements with OOPS on the two existing satellites and/or the original North-Hall support. We do not require the gantry support for OOPS if it is not available.

Tab. 1 shows the measured and projected properties of both OHIPS and OOPS. In the following, we will breifly discribe the particle identification.

| | $\Delta p/p$ | $\delta p/p$ | $\delta\theta, \delta\phi$ | drift | $\Delta\Omega$ | drift (optional) | $\Delta\Omega$ (optional) |
|---|---|---|---|---|---|---|---|
| OHIPS | ±4% | 0.2% | 1 mr | 2.0 m | 4.0 msr | 1.0 m | 16.0 msr |
| OOPS | ±10% | 0.5% | 1 mr | 1.4 m | 1.3 msr | 0.7 m | 5.2 msr |

Table 1: Properties of OHIPS and OOPS.

The OHIPS focal plane instrumentation has been recently upgraded to optimize it for electron detection. A new gas cherenkov, a second VDCX drift chamber, a third scintillator and an array of lead glass shower counters have been added.

The OOPS focal plane contains 3 HDC drift chambers and 3 backing scintillators. The scintillators are of two thicknesses: the first one is 1.6 mm thick, while the second and third are 4.8 mm thick. The scintillators have photomultiplier tubes on each end ("left" and "right"). A multiple coincidence is formed among their signals to generate the OOPS trigger, timing and particle identification.

Fig. 5 shows a typical correlation spectrum of the OOPS scintillators from single arm $^{12}$C(e,X$^+$) data with a central momentum of 436 MeV/c. Here, "ΔE"-detector represents the first layer scintillator, while the "E"-detector is the sum of the scond and third scintillator. The left and right ADCs for each layer are summed and averaged. In this case, most of deuterons are stopped in the third scintillator and protons and $\pi^+$ penatrate through. Clearly, deuterons can be well indentified in the spectrum.

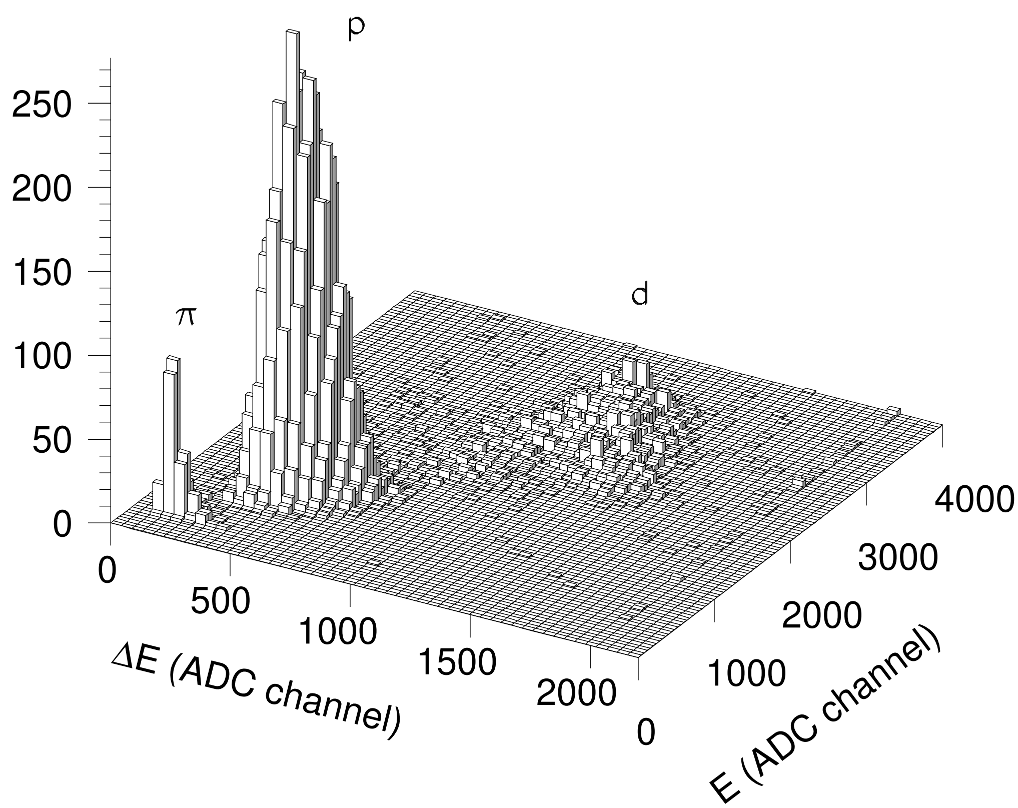


Figure 5: Spectrum of OOPS focal plane scintillators from $^{12}$C(e,X$^+$) reactions showing the particle identification of $\pi^+$, protons and deuterons.

In the summer of 1996, optics data were obtained for 3 OOPS and the reconfigured OHIPS using beam energies of 200 and 345 MeV. In each spectrometer complete momentum scans were performed for point and extended target configurations, with and without sieve slits. With a 660 MeV beam a maximum OOPS operating instantaneous luminosity of about $2\times10^{38}$ cm$^{-2}$s$^{-1}$ was observed. The OOPS was tuned to protons in the (300–500) (MeV/c) range and positioned as forward as $20^0$ with respect to the beam direction. With the same beam we performed $^1$H$(e, e'p)$ coincidence studies between OHIPS and each of the three OOPS, and we carried out a set of short $^{12}$C$(e, e'p)$ measurements with two pairs of OOPS. Finally, with a 40% polarized beam, we performed a $^{12}$C$(\vec{e}, e'p)$ commissioning experiment which is currently being analyzed as a Ph.D. dissertation.

From Dec. 1996 to early Feb. 1997, we have successfully carried out a long experiment run. During this run we accomplished a systematic and extensive program of precise measurement of the $^2$H$(\vec{e}, e'p)$ interference structure functions $R_{LT}$, $R'_{LT}$ and $R_{TT}$ with a polarized beam and consequently with two OOPSs and three OOPSs in coicidence with OHIPS [27, 28, 29]. The data are currently being analyzed as three Ph.D. dissertations.

## 3.2 Polarized beam

The polarized electron source being used in experiments at Bates is under development and operated by a group led by M. Farkhondeh. The source is able to deliver currents in excess of 50 $\mu$A with a polarization of approximately 0.40. Stabilities of the current and polarization over helicity flips can be better than $10^{-5}$ and thus exceed the requirements of this proposed experiment by several orders of magnitude. We assume that operation of the source will be stable and therefore in our count rate estimate we make no provision for down time due to source problems.

This has been shown in the OOPS commissioning experiments. For example, in the $^{12}$C$(\vec{e}, e'p)$ experiment, a stable beam with currents more than 10 $\mu$A and polarization in the range of 37-40% has been delievered in the B-line for over a month.

The development of high polarization source based on strained GaAs crstals will be highly beneficial to our proposed measurements. Since the experimental asymmetries $A_{exp} = P_{beam} \cdot P_{target} \cdot A_{x,z}$, a factor of 2 increase in the beam polarization would improve the measurements in the figure of merit by a factor of 4.

The beam polarization will be monitored with the South Hall B-line Möller polarimeter. Based on the OOPS run experience, one Möller measurement takes typically about one hour. This can be done periodically throughout the running period. Currently, the typical signal-to-noise ratio in detecting the Möller electrons is about 2.5 and the measurement error of the polarization is $\pm 5\%$.

Besides the Möller polarimeter, we plan to use one OOPS to detect elastically scattered electrons at a forward angle to monitor the product of the polarization of the beam and target. We will describe it in detail in Sec. 3.4.

Based on the count rate and the trues/accidentals ratio estimates, we conclude that a pulsed beam with about 1% duty factor will be feasible for this experiment. However, with the nice features of an extracted CW beam, we believe we could improve the figure of merit in the measurements. Therefore, we would like to use a CW beam if it is available.

## 3.3 Polarized $^3\vec{\mathrm{He}}$ target

We plan to use the high pressurized polarized $^3$He target contributed by the collaboration of Exp 88-25.

The polarized $^3$He target is based on spin exchange with laser optically pumped Rb vapor. This technology has been developed over the past 10 years by T. Chupp and collaborators, and most recently been used in very successful experiments at SLAC E-142 and E-154. The detailed description of the target can be found in the proposal and updates of Exp 88-25. In the following, we briefly listed the specifications of the target:

- **Target length**: 10 cm total / 8 cm visible to detectors
- **Target density**: $2.7 \times 10^{20}$ cm$^{-3}$ (10 atmospheres)
- **Other species**: $N_2$ – $2.5 \times 10^{18}$ cm$^{-3}$ (60 torr)
- **Target cell diameter**: 2 cm
- **Polarization**: 50%
- **Beam current**: 5-10 $\mu$A
- **Material**: glass (Corning 7056)
- **Electron windows**: 0.01 cm glass, Helium gas cooled
- **Side walls**: 0.07 cm glass
- **Laser power**: 30-45 Watts from Fiber Coupled Laser Diode Arrays (795 $\pm$ 0.1 nm)

Since only about a 4 cm target length is visible to OOPS, the useful luminosity will be about $6.8 \times 10^{34}$ cm$^{-2}$·s$^{-1}$ with a 10 $\mu$A beam current.

During the experiment, the target spin direction is aligned parallel to (for $A_z$ asymmetry) or perpendicular to (for $A_x$ asymmetry) the direction of momentum transfer as shown in Fig. 4c. A pair of Helmholtz coils provides the necessary quantization axis by supplying a holding field of about 3 mT.

Background events from the target entrance and exit windows do not contribute because electrons from the thin cell windows will be outside the shielded spectrometer acceptances. The target polarization and the dilution factor (the ratio of the number of coincidence events from $^3$He to the total number of events for a given kinematics) enter the analysis. In this case, the dilution factor is mostly caused by nitrogen, which can be measured and subtracted with an equivalent target of the same geometry. However, we do not expect a significant contribution to the $^3\vec{\mathrm{He}}(\vec{e}, e'd)p$ measurements. The target polarization will be determined by the NMR measurements (refer to Exp 88-25 proposal [4]). Furthermore, we plan to use one OOPS to detect elastically scattered electrons at a forward angle to monitor the polarization of the beam and target. We will describe this in detail next.

## 3.4 $\vec{e}$ - ${}^3\vec{\mathrm{He}}$ elastic scattering as a polarization monitor

In this section we discuss the possibility of measuring the product of the beam and the target polarizations directly by measuring the asymmetry in the elastic electron scattering cross section. This method provides, in effect, a continuous monitor of the polarizations of the beam and of that region of the target through which the beam passes.

The asymmetry for scattering off a polarized $^3$He target is given by [30]:

$$A_{elas} = \frac{\Delta}{\Sigma} = -\frac{v'_T F_T^2 \cos\theta^* + 2v'_{TL} F_T F_L \sin\theta^* \cos\phi^*}{v_L F_L^2 + v_T F_T^2}, \tag{3}$$

where the $v_K$ are kinematical factors, $\theta^*$ is the angle between the target spin and $\mathbf{q}$, $\phi^*$ is the angle between the scattering plane and the reaction plane, and $\Sigma$ and $\Delta$ are the spin-independent and spin-dependent parts of the cross section, respectively. We assume that the charge and magnetic form factors are normalized such that:

$$F_c(Q^2) = F_m(Q^2) = 1, \text{ for } Q^2 = 0 \tag{4}$$

and so:

$$Z^2 F_c^2 = 4\pi \frac{F_L^2}{(1+\tau)} \tag{5}$$

$$\mu_A^2 F_m^2 = 4\pi \frac{F_T^2}{2\tau}, \tag{6}$$

where $\mu_A = \frac{M_T}{m_N}\mu(^3\mathrm{He})$ = -6.368 nm and $\tau = Q^2/4M_T^2$. Since the elastic charge and magnetic form factors are accurately known for $^3$He for the proposed kinematics, the measured elastic asymmetry can be used to determine the product of beam and target polarization.

Next we estimate the precision of this method. We consider elastic scattering from the polarized $^3$He target at 750 MeV electron beam energy. We propose to detect elastically scattered electrons at 20° by using one OOPS. This OOPS will view the central 8 cm of the target. Thus, the luminosity is $\approx 1.4 \times 10^{35}$ cm$^{-2}$s$^{-1}$. The solid angle for electron scattering is 1.3 msr. At 20°, the elastic $e-{}^3$He cross-section is about $5.6 \times 10^{-30}$ cm$^2$/sr. Since the polarization measurements will be done parasitically during the asymmetry $A_{x,z}$ measurements for the ${}^3\vec{\mathrm{He}}(\vec{e}, e'd)p$ reaction, elastical $\theta^*$ will not be at its optimal value around 100°. This will reduce $A_{elas}$ to about 0.035 during both $A_x$ and $A_z$ measurements. Consequently, with a 40% polarized electron beam and a 50% polarized target, the polarization product will be measured to ±8% in about 1 hour.

Besides the elastic scattering monitor, we plan to measure the beam polarization by using the South Hall Möller polarimeter setup and the target polarization and dilution factor by using the NMR technique. This can be done continuously in a reasonable time intervals and will give an independent method to measure the beam and target polarization for a consistency check.

# 4 Beam time request

The proposed kinematics and the estimated count rates are shown in Table 2 and 3. The estimate of counting rates and statistical uncertainties were based on one OOPS and OHIPS configuration and were calculated using MCEEP [31]. The luminosity assumed is $7 \times 10^{34}$ cm$^{-2}$·s$^{-1}$ with a 10 $\mu$A beam current. The measured $^3$He$(e, e'd)p$ momentum distribution from NIKHEF and the off-shell e-d cross-section [32] are incorporated into MCEEP, thus the rates as well as the beam time estimates are considered to be very realistic. We intend to run immediately after Exp 88-25. Therefore, we do not expect over-head time such as for the target installation and etc.

We intend to use one OOPS at a 0.7 m drift distance and emphasize only the parallel kinematics. The OOPS central momenta are set at 400 and 490 MeV/c so that the central recoil momenta are at 20 and 110 MeV/c, resepectively. This can be done by simply changing the OOPS dipole field and no angle change is required. In this way, the emphasis of the measurements is given to the two interested recoil momentum regions. If two OOPS modules are used, then the perpendicular kinematics will be emphasized. The results of the experiment will be similar. However, The acceptance will be reduced due to the requirement of a miniumal 20° separation angle at a 1.4 m drift distance.

| | | Singles | | | | Accidentals |
|---|---|---|---|---|---|---|
| | central kinematics | $(e, e')$ (Hz) | $(e, d)$ (Hz) | $(e, p)$ (Hz) | $(e, \pi^+)$ (Hz) | $(e, e'd)$ (hr$^{-1}$) |
| OHIPS | $\theta_e = 30.0°$<br>$e' = 706$ MeV/c | 168 | | | | |
| OOPS KIN1 | $\theta_d = 68.6°$<br>$P_d = 400$ MeV/c<br>$P_r = 20$ MeV/c | | 669 | 157 | 16 | 80 |
| OOPS KIN2 | $\theta_d = 68.6°$<br>$P_d = 490$ MeV/c<br>$P_r = 110$ MeV/c | | 167 | 75 | $\sim$0 | 20 |

Table 2: Proposed kinematics with a 750 MeV electron beam and estimates of singles and accidentals rates.

| $P_r$ (MeV/c) | Count/hour | $\delta A_x$ | $\delta A_z$ | beam time (hrs) | total (hrs) |
|---|---|---|---|---|---|
| 20 | 5369 | 0.0076 | 0.0076 | 2×80 | |
| 110 | 1231 | 0.0116 | 0.0116 | 2×150 | 460 |

Table 3: Estimates of event count-rates and statistical errors at a given beam time.

The estimated singles count rates and accidental coincident rates are also shown in Table 2. The singles count rates (those observed in OHIPS originating from the $(e, e')$ reaction and in OOPS originating from $(e, p)$ and $(e, \pi^+)$ reactions) are estimated with the computer codes QFS and EPC of Lightbody and O'Connell [33]. The singles count rates in OOPS originating from the $(e, d)$ reaction are estimated by using the above described

$(e, e'd)$ Monte Carlo method and integrating the rates over a large acceptance for scattered electrons. Accidental coincidence rates were calculated assuming a coincidence timing width of 2 ns and a duty factor of 1%. The listed accidental rate is over the whole missing energy range within the momentum acceptances of the spectrometers. Since the deuterons detected in OOPS can be well-selected with the particle identification, accidentals rates caused by $(e, p)$ and $(e, \pi^+)$ reactions are not included. When the reaction $^3\mathrm{He}(e, e'd)p$ is selected, a cut on the two-body breakup peak is applied. The accidentals within the cut will be about a factor of ∼20 less than the listed numbers. As shown in Table 2, the accidental coincidence rate is insignificant compared to the true coincident rates.

The experimental asymmetries $A^{\mathrm{exp}}_{x,z}$ are the products of $A_{x,z}$ and polarizations of beam and target, as shown in Eq. 7:

$$A^{\mathrm{exp}}_{x,z} = P_{\mathrm{b}} \cdot P_{\mathrm{t}} \cdot A_{x,z} \,. \tag{7}$$

Thus, the statistical errors will be amplified by the factor of $1/(P_{\mathrm{b}} \cdot P_{\mathrm{t}})$, which is approximately 5 with a 40% polarized beam and a 50% polarized target. The final statistical errors are shown in Tab. 3. Since the statistical errors dominate, systematic errors caused by the uncertainties in the polarization of beam (∼5%) and target ($\lesssim$ 5%) are currently not included in the estimates. The quality of proposed measurements is shown early in Fig. 2 and 3. Note that, if physics issues arise with our data, possible measurements with perpendicular kinematics and/or with the out-of-plane capability for $\mathrm{A}_y$ as well as measurements of other reaction channels can be considered thereafter, as we discussed at the end of Sec. 2.

# 5 Responsibilities

From the Summer 1996 to February 1997, the modified OHIPS spectrometer and a set of three OOPS spectrometers have been commissioned and successfully used in the $^{12}\mathrm{C}(\vec{e}, e'p)$ and $^{2}\mathrm{H}(\vec{e}, e'p)$ coincidence experiments with beam energies at 660 MeV and 800 MeV, respectively. Presently, OHIPS is operated at a 1.8 m drift distance and OOPS at a 1.4 m drift distance.

Similar to Exp 88-25, we would like to maximize the angular acceptance in OHIPS. That is, we intend to operate OHIPS at about 1.0 m drift distance. We anticipate that OHIPS will be commissioned in this operation mode before Exp 88-25 data-taking. Since the angular acceptance can be increased by a factor of 4 by running OOPS with a drift distance of 0.7 m instead of 1.4 m, both Exp 88-25 and this proposed experiment intend to operate OOPS in such way. Therefore, we foresee a joint effort from Bates Laboratory, the OOPS collaboration and the collaboration of Exp 88-25 in commissioning both OHIPS and OOPS at an adequate time prior to any experimental data-taking.

We intend to make use of the polarized $^3\mathrm{He}$ target contributed from Exp 88-25. Besides operating the target, we do not anticipate the need for any additional hardware development for the target.

The collaboration has experience of running OHIPS and OOPS in both single arm and coincidence modes and also has experience of running the South Hall Möller polarimeter. After Exp 88-25, we will also have an operational polarized $^3$He target. We will benefit from the analysis software used in the present OOPS collaboration. We have preliminarily identified two students (M. Wu and A. Skabelin) from MIT who can be Ph.D. candidates doing dissertation on this proposed experiment. Dr. S. Nagorny will provide necessary calculations in the $^3\vec{\mathrm{He}}(\vec{e}, e'd)p$ reaction channel and will look into possible physics options in the (semi-)inclusive $^3\vec{\mathrm{He}}(\vec{e}, e'p)$X (X=d,pn) reaction [23].

In a summary, this proposed experiment requires no additional hardware development and resources, only beam time.

# References


[1] Blankleider and R.M. Woloshyn, Phys. Rev. C 29, 539 (1984).

[2] R.G. Milner, *Proceedings of the Workshop on Polarized $^3$He Beams and Targets*, edited by R.W. Dunford and F.P. Calaprice (AIP 131, New York, 1984) p. 186.

[3] H. Gao *et al.*, Phys. Rev. C 50, R546 (1994).

[4] Bates proposed-approved experiment 88-25, spokespersons: A. Bernstein, T. Chupp and R. Milner, "Quasielastic polarized electron scattering from polarized $^3$He", (1988).

[5] M. Meyerhoff, D. Eyl, A. Frey *et al.* (Mainz-A3 Collab.), Phys. Lett. B 327, 201 (1994).

[6] NIKHEF experiment 94-05, spokespersons: J.F.J. van den Brand and C.W. de Jager, "Measurement of quasi-elastic spin-dependent electron scattering from a polarized $^3$He internal target", (1994).

[7] MAMI experiment A1/95-4 at Mainz, "Measurement of the neutron electric form factor via $^3\vec{\mathrm{He}}(\vec{e}, e'n)$ ", (1995).

[8] BLAST proposal at the South Hall Ring of the MIT-Bates Linear Accelerator Center, 1991 (unpublished); Workshop on *Electronuclear Physics with Internal Targets and the BLAST Detector*, Tempe, Arizona, March 1992, eds. R. Alarcon and M. Butler, (World Scientific, Singapore, 1993).

[9] TJNAF proposed-approved experiment E-95-001, spokesperson: H. Gao, "Precise measurements of the inclusive spin-dependent quasi-elastic transverse asymmetry $A_{T'}$ from $^3\vec{\mathrm{He}}(\vec{e}, e')$ at low $Q^2$", (1995).

[10] P.L. Anthony *et al.*(SLAC-E142 Collab.), Phys. Rev. Lett. 71, 959 (1993).

[11] SLAC proposed-approved experiment E-154, spokesperson: E.W. Hughes, (1993).

[12] HERMES experiment at DESY, see HERMES collaboration, DESY Report No. DESY-PRC-93-06, 1993 (unpublished).

[13] J.L. Friar *et al.*, Phys. Rev. C 42, 2310 (1990).

[14] R.W. Schulze and P.U. Sauer, Phys. Rev. C 48, 38 (1993).

[15] J. Friar, in *Electronuclear Physics with Internal Targets and the BLAST Detector*, eds. R. Alarcon and M. Butler, (World Scientific, Singapore, 1993), p. 210.

[16] J.L. Friar, B.F. Gibson, C.R. Chen and G.L. Payne, Phys. Lett. B 161, 241 (1985).

[17] J.-M. Laget, Phys. Lett. B 276, 398 (1992).

[18] S. Nagorny and W. Turchinetz, "Manifestation of Small Nuclear Components and Current Structure in the $^3$He$(e, e'd)p$ Reaction", Accepted for publication on Phys. Lett. B, (1996).

[19] S. Nagorny, to be submitted for publication, (1997).

[20] I. Sick, private communication.

[21] TJNAF proposal PR-94-020, spokespersons: W. Korsch, R. McKeown and Z.-E. Meziani, "Investigation of the $^3$He wave function using the $^3\vec{\mathrm{He}}(\vec{e}, e'p)d$ and the $^3\vec{\mathrm{He}}(\vec{e}, e'p)pn$ reactions", (1994).

[22] TJNAF proposal PR-94-023, spokesperson: F.W. Hersman, "Measurement of small components of the $^3$He wave function using $^3\vec{\mathrm{He}}(\vec{e}, e'p)$ in Hall A", (1994).

[23] S. Nagorny, private communication.

[24] C. Tripp *et al.*, Phys. Rev. Lett. 76, 885 (1995).

[25] P.H.M. Keizer *et al.*, Phys. Lett. B 157, 255 (1985).

[26] D.C. Carey, TURTLE: computer program for simulating charged particle beam transport systems, Fermilab National Accelerator Laboratory, NAL-64, (1978).

[27] Bates experiment 89-10, spokesperson: R. Alarcon, "Measurement of the $(\vec{e}, e'p)$ electrodisintegration of the deuteron", (1989).

[28] Bates experiment 89-14, spokespersons: W. Bertozzi *et al.*, "A program to determine the five deuterium $(\vec{e}, e'p)$ response functions $(f_{\mathrm{L}}, f_{\mathrm{T}}, f_{\mathrm{LT}}, f_{\mathrm{TT}}, f'_{\mathrm{LT}})$", (1989).

[29] R. Alarcon and Z.-L. Zhou, A memorandum to Prof. S. Kowalski, Director, Bates Linear Accelerator Center from the OOPS collaboration, "Upcoming deuteron measurements with the OOPS system", (Nov. 5, 1996).

[30] T.W. Donnelly and A.S. Raskin, Ann. Phys. 169, 247 (1986).

[31] P.E. Ulmer, computer program MCEEP, TJNAF Tech. Note 91-101, (1991).

[32] R. Ent, Ph.D. Dissertation, Vrije Universiteit, Amsterdam, (1989); private communication.

[33] J. Lightbody and J.S. O'Connell, Computers in Physics 2, 57 (1988).